Available online at www.sciencedirect.com

SCIENCE DIRECT®

Journal of Molecular Catalysis A: Chemical 202 (2003) 215–227

JOURNAL OF MOLECULAR CATALYSIS A: CHEMICAL

www.elsevier.com/locate/molcata

Interaction of thiophene with stoichiometric and reduced rutile TiO_2(1 1 0) surfaces: role of Ti^{3+} sites in desulfurization activity

Gang Liu [a], José A. Rodriguez [a,*], Jan Hrbek [a], Brian T. Long [b], Donna A. Chen [b]

[a] *Department of Chemistry, Brookhaven National Laboratory, P.O. Box 5000, Upton, NY 11973, USA*
[b] *Department of Chemistry and Biochemistry, University of South Carolina, Columbia, SC 29208, USA*

Received 13 January 2003; accepted 10 March 2003

Abstract

The adsorption of thiophene (C_4H_4S) on almost stoichiometric TiO_2(1 1 0) and defective TiO_{2-x}(1 1 0) surfaces has been studied with a combination of synchrotron-based high-resolution photoemission spectroscopy, thermal desorption mass spectrometry (TDS), and first-principles density-functional (DF) slab calculations. The bonding nature between C_4H_4S and Ti or O sites of TiO_2(1 1 0), and point defects (oxygen vacancies) of TiO_{2-x}(1 1 0) was investigated. Over an almost stoichiometric TiO_2(1 1 0) surface, the adsorption and desorption of C_4H_4S is completely reversible. In the submonolayer regime, four adsorption states in the temperature range of 150–450 K were identified in TDS. No thiophene decomposition was observed up to 800 K under ultra-high vacuum (UHV) conditions. The results of DF calculations indicate that at small coverage the molecule should be bonded with its ring nearly parallel to the surface. At high coverages of thiophene, bonding through the S atom becomes more stable because it reduces adsorbate ↔ adsorbate repulsion. On a defective TiO_{2-x}(1 1 0) surface with ∼45% of Ti^{3+} and Ti^{2+}, a small fraction of the adsorbed thiophene molecules (<0.05 ML) decomposed. Our experimental and theoretical studies indicate that the vacancy states of TiO_{2-x}(1 1 0) interact poorly with the LUMO of thiophene. This is a behavior opposite to that found for the adsorption of S_2, CH_3S and SO_2. The role of Ti^{3+} sites in the desulfurization activity of MoS_x/TiO_2 catalysts is analyzed in light of these results.

Keywords: Adsorption; TiO_2(1 1 0); Thiophene; TDS; XPS; Density-functional theory; Desulfurization

1. Introduction

As a typical organosulfur compound, thiophene (C_4H_4S) has been extensively studied on model or real catalyst surfaces to understand the details of the industrially important hydrodesulfurization (HDS) process [1]. In modern petroleum refining operations, sulfur is removed over alumina supported molybdenum and cobalt sulfide catalysts in order to prevent poisoning of catalysts used downstream for the reforming of hydrocarbons [2], and reduce the amount of sulfur oxides released into the atmosphere during the combustion of gasoline and other fuels [3]. More stringent environmental regulations have driven extensive research in modifying existing HDS catalysts or developing new ones for more efficient catalytic processes [1]. It is well known that sulfur typically exists in crude oil in the form of thiols, sulfides, and thiophenes, among other compounds [2]. Since thiophene and its derivatives are the most difficult compounds to desulfurize [2], the focus has been on the chemistry of thiophene over transition metals [4–9], oxide supported catalysts

* Corresponding author. Tel.: +1-631-344-2246; fax: +1-631-344-5815.
E-mail address: rodrigez@bnl.gov (J.A. Rodriguez).

1381-1169/03/$ – see front matter © 2003 Elsevier Science B.V. All rights reserved.
doi:10.1016/S1381-1169(03)00206-1

[10–13], and metal sulfides [1,6,14]. On transition metal surfaces such as Mo(1 1 0) [4,6] or Mo(1 0 0) [5], complete thiophene decomposition to S and C_xH_y fragments was observed at temperatures below 300 K. In contrast, on alumina supported sulfided Mo catalysts [12,13], thiophene is only weakly chemisorbed, and no reactivity was observed either under ultra-high vacuum (UHV) conditions or a 9.5 Torr thiophene partial pressure up to 693 K. In spite of the use of oxides as catalysts/absorbents in HDS operations [2], little is known about the fundamental chemistry of thiophene on pure and well-defined oxide surfaces [15,16]. On a polycrystalline ZnO surface, thiophene was weakly chemisorbed, and mostly desorbed at temperatures below 250 K [15]. A very small fraction of the adsorbed C_4H_4S (∼0.02 ML) that interacts with O-unsaturated Zn sites was decomposed [15]. Previous studies show that on high surface area γ-Al_2O_3 powders, thiophene interacts only weakly with the substrate, and no decomposition of the molecule was observed up to 600 K under UHV conditions or a partial thiophene pressure of 3.0 Torr [16].

In another area of research, self-assembled monolayers (SAMs) formed by organosulfur compounds on metal [17], semiconductor [18], and oxide [19] single crystal surfaces are receiving much attention due to possible technical applications in areas of biosensing, catalysis, tribology, and microelectronics. Emphasis has been on the nature of the interactions between the substrates and S-containing groups in the monolayer interface, including the identification of sites for molecular adsorption and dissociation, and the possible formation of lateral S–S bonds. One of the key issues is the formation of the interfacial chemisorption bond (the "electrical junction" in practical terms), which is closely related to the electron transfer between semiconductor particles and molecular wires [18]. Most work has concentrated on alkanethiol-derived SAMs [20]. Investigations also involve π-conjugated sulfur-containing molecules on metal surfaces and semiconductors [21,22], perhaps as the most promising application in the fabrication of microelectronic devices [21,22]. Recent studies show that thiophene when present in solutions strongly chemisorbs on Au(1 1 1) thin films during the self-assembly process at room temperature [22].

In this work, we study the surface chemistry of thiophene on stoichiometric TiO_2(1 1 0) and defective TiO_{2-x}(1 1 0) using synchrotron-based high-resolution X-ray photoemission spectroscopy (XPS), thermal desorption mass spectrometry (TDS), and first-principle density-functional (DF) slab calculations. The rutile TiO_2(1 1 0) surface is considered to be one of the prototypical systems for an oxide [23], and is an ideal system to study the role of surface defects on the chemical and catalytic properties of an oxide [24,25]. In the chemical industry, titania is employed for trapping S-containing impurities in oil-derived feedstocks, and as a catalyst for the Claus process [2,26]. In addition, titania has been shown to be an "active" support for Mo-based HDS catalysts [27–29]. It was found that TiO_2 supported Mo catalysts exhibited 4.4 times higher HDS activity than the γ-Al_2O_3 supported ones [27]. Among a number of possible explanations for the observed high activities, it has been suggested that Ti^{3+} species act as "electronic promoters" [29], but their possible role in C–S bond cleavage needs further investigation [27–29]. Recent studies show that oxygen vacancies (related to $Ti^{\delta+}$, $\delta \leq 3$) in TiO_2(1 1 0) play an important role in adsorbing and dissociating the SO_2 molecule [24]. For CH_3SH adsorption on TiO_2(1 1 0) surfaces with a large number of oxygen vacancies and defects, the C–S bond breaks in the 250–750 K temperature range with CH_3 or CH_4 desorbing into gas phase, leaving S and CH_x fragments on the surfaces [19]. Since thiophene and its derivatives are the most difficult compounds to desulfurize [1,2], it is interesting to elucidate the role of oxygen defects and Ti^{3+} species in the adsorption and dissociation of thiophene. To the best of our knowledge, this is the first systematic study examining the interaction of thiophene with a well-defined oxide surface.

2. Experimental and theoretical methods

2.1. Experimental methodology

The experimental work was carried out in two separate UHV chambers. The photoemission experiments were performed in a UHV chamber [17] at the U7A beamline in the National Synchrotron Light Source (NSLS) at Brookhaven National Laboratory. This chamber (with a base pressure of $\sim 5 \times 10^{-10}$ Torr) is fitted with a hemispherical electron energy analyzer

with multichannel detection, optics for low-energy electron diffraction (LEED), a quadrupole mass spectrometer (QMS), and a twin (Mg Kα and Al Kα) X-ray source. The combined energy resolution in the synchrotron experiments was 0.3–0.4 eV. The binding energy (BE) values were determined with respect to the Fermi level. The TDS experiments were done in a second UHV chamber [24] (with a base pressure of $\sim 5 \times 10^{-10}$ Torr), which is equipped with a hemispherical electron energy analyzer with single channel detection, a twin X-ray source, and a residual gas analyzer (SRS-RGA). The residual gas analyzer was surrounded by a stainless steel jacket with a 10 mm aperture and a differential pumping system for TDS measurements. All the TDS spectra reported in Section 2 were collected at a heating rate of 2 K/s.

The TiO_2(1 1 0) single crystal was sandwiched between Ta plates that were spot-welded to two Ta heating legs of a manipulator [19,24]. The sample could be cooled as low as 100 K by thermal contact with a liquid nitrogen reservoir and resistively heated to 1200 K. The temperature was monitored by a type C thermocouple spot-welded on the Ta plate edge. Prior to each experimental the TiO_2(1 1 0) crystal was cleaned by repeated cycles of 1 keV Ne^+ ion bombardment followed by heating at 950 K until no impurities were detected by XPS [19]. After this treatment, the sample exhibited a sharp (1 × 1) LEED pattern. Defective surfaces were created by Ne^+ bombardment at 1 keV for 2 min [23,24]. High-purity (99%) thiophene (Aldrich) was further purified by several freeze-pump-thaw cycles with liquid nitrogen prior to dosing. The dosing was performed through a leak valve with a stainless tube directed to the sample surface. Mass spectrometry indicated that thiophene did not decompose in the gas handling system or on the walls of the UHV system.

2.2. First-principles density-functional calculations

The geometries and bonding energies for thiophene on stoichiometric and partially reduced TiO_2(1 1 0) were calculated using the Cambridge serial total energy package (CASTEP) code [30,31]. Previous work indicates that CASTEP can be quite useful for studying adsorption processes on TiO_2(1 1 0) [19,32–34] and other oxide surfaces [35–37]. CASTEP was recently used to examine the interaction of sulfur and methanethiol with titania [19,32]. In this code, the Kohn–Sham equations are solved within the framework of density-functional theory by expanding the wave functions of valence electrons in a basis set of plane waves with kinetic energy smaller than a specified cut-off energy, E_{cut} [30,31]. The presence of tightly-bound core electrons was represented by non-local ultra-soft pseudopotentials of the Vanderbilt-type [38]. The valence s and p states of C, O and S, and the semicore (3s, 3p) and valence (3d, 4s, 4p) states of Ti were explicitly treated. Reciprocal-space integration over the Brillouin Zone was approximated through a careful sampling at a finite number of *k*-points using the Monkhorst-Pack scheme [39]. In all the calculations, the kinetic energy cut off ($E_{cut} = 400$ eV) and the density of the Monkhorst-Pack *k*-point mesh (a 8 × 4 × 1 grid for the smallest (1 × 1) surface unit cell, reduced to 4 × 4 × 1 or 4 × 2 × 1 grids for larger cells) were chosen high enough in order to ensure convergence of the computed structures and energetics. The exchange-correlation contribution to the total electronic energy is treated in a generalized gradient corrected (GGA) extension of the local density approximation (LDA) [40]. We have used the GGA functional in the form proposed by Perdew et al. [41]. This functional should give reasonable predictions for the bonding energies of thiophene on TiO_2(1 1 0) according to previous studies for the chemisorption of S-containing species [19,32]. For the bonding of small molecules like CO and NO to TiO_2(1 1 0), the Perdew-Wang functional predicts adsorption energies that are within 5 kcal/mol of the experimental values [33,34]. In this work, our main interest is in relative energy changes with adsorption site, adsorbate configuration and coverage, not in absolute values.

The structural parameters of the thiophene/TiO_2 (1 1 0) and thiophene/TiO_{2-x}(1 1 0) systems in their different configurations were determined using the Broyden-Fletcher-Goldfarb-Shanno (BFGS) minimization technique, with the following thresholds for the converged structures: energy change per atom less than 5×10^{-6} eV, residual force less than 0.02 eV/Å, and the displacement of atoms during the geometry optimization less than 0.001 Å. For each optimized structure, the partial charges on the atoms were estimated by projecting the occupied one-electron eigenstates onto a localized basis set with a subsequent Mulliken population analysis [42]. The Mulliken charges must not be interpreted in absolute

quantitative terms because of the uncertainty in uniquely defining a charge-partitioning scheme [42].

3. Results

3.1. Adsorption of thiophene on TiO_2(1 1 0) and TiO_{2-x}(1 1 0): TDS and XPS studies

Fig. 1 displays typical TDS spectra for thiophene adsorption on an almost stoichiometric TiO_2(1 1 0) surface following a series of exposures at 100 K. For each set of experimental data in Fig. 1, the crystal was prepared with an identical treatment, as described in Section 2.1. Previous studies [43] show that the sample preparation used in the present work leads to a limited number of surface point defects (oxygen vacancies, <7%). The most intense parent ion signal, $m/z = 84$ atomic mass units (amu), of the thiophene molecule was monitored. C_4H_4S was the only detectable desorption product. No other hydrogen-containing products (H_2, C_4H_6, and C_4H_8) or sulfur-containing species (S, S_2, and SO_2) were observed, indicating that the desorption process is exclusively molecular. After desorption, no carbon and sulfur residues were left on the surface, as evidenced by high-resolution XPS (see the following Figs. 2 and 3). It is well known that absolute coverages for adsorbates on TiO_2 surfaces are generally difficult to determine [44]. In this work, the integrated area of each TDS spectrum was used to determine the relative monolayer (ML) coverage and in Fig. 1 the spectra are plotted as a function of this parameter.

A complex behavior is seen when the thiophene coverage changes. For 0.04 ML thiophene adsorption, two very weak desorption peaks appear, labeled as α_1 and α_2, with peak maxima (T_{max}) at 450 and 320 K, respectively. The α_1 desorption state can be attributed to thiophene adsorption on defects of the surface since this state is rapidly saturated with increasing thiophene exposure [17]. At 0.7 ML of adsorption, a third peak

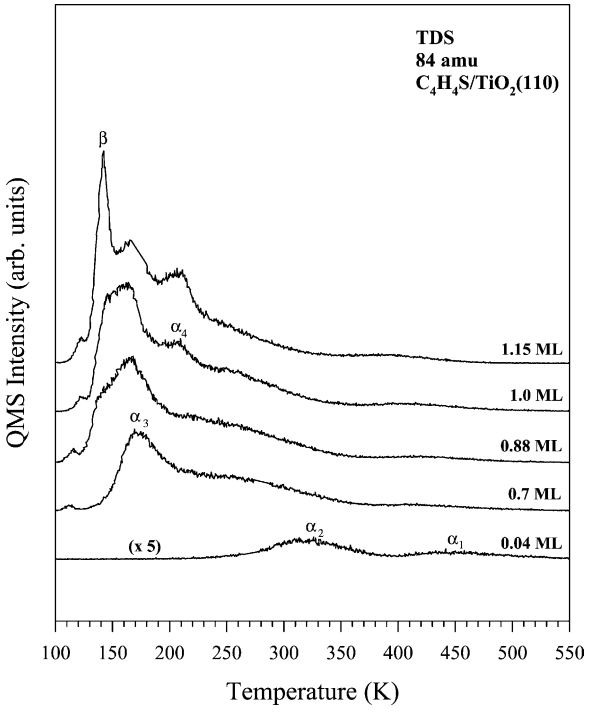

Fig. 1. Thermal desorption spectra for thiophene adsorption on an almost stoichiometric TiO_2(1 1 0) surface at 100 K as a function of coverage relative to a monolayer. The ion signal (84 amu) was monitored. The heating rate was 2 K/s.

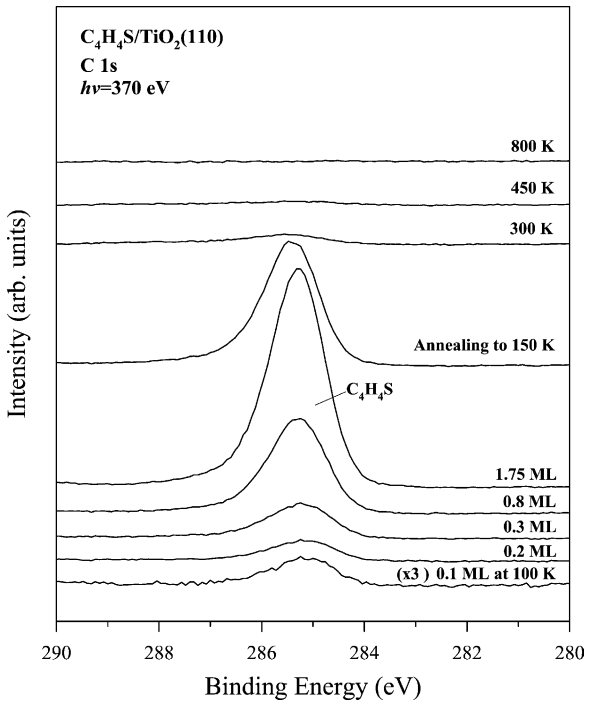

Fig. 2. C 1s spectra ($h\nu = 370$ eV) for the adsorption of C_4H_4S on an almost stoichiometric TiO_2(1 1 0) surface. C_4H_4S was dosed at 100 K, and the surface was annealed to the indicated temperatures.

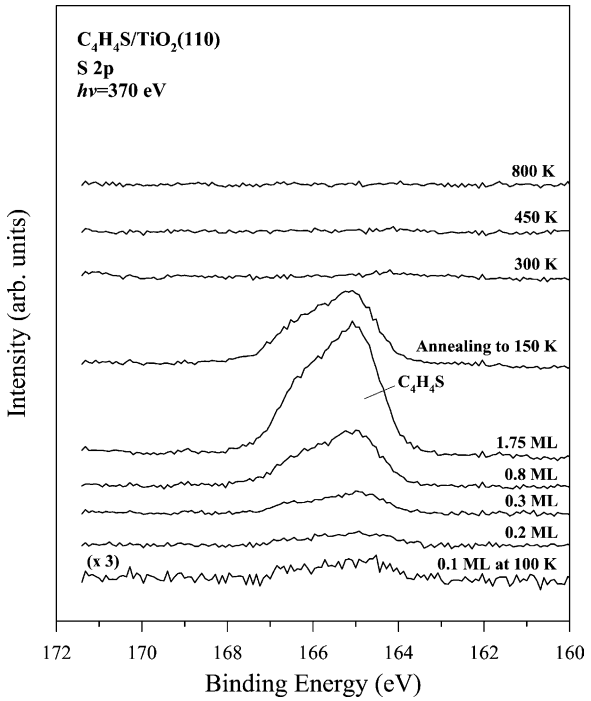

Fig. 3. S 2p spectra ($h\nu = 370$ eV) for the adsorption of C_4H_4S on an almost stoichiometric TiO_2(1 1 0) surface of Fig. 2. C_4H_4S was dosed at 100 K, and the surface annealed to the indicated temperatures.

appears at 170 K, labeled as α_3, with α_1 and α_2 at 420 and 265 K, respectively. The shifting to lower temperatures with increasing exposures for desorption states implies repulsive interactions between the adsorbates [19]. As the exposure increases, a fourth peak (α_4) is seen at 205 K. At 1.15 ML, a relatively sharp peak (β) appears at 140 K, grows without saturation, and is assigned as the condensed multilayer desorption. The desorption temperature for β is consistent with the previously found on Cu(1 1 1) [46], Ag(1 1 1) [47], and Au(1 1 1) [17]. A relatively small peak at ca. 120 K is probably an artifact of our experimental set-up. On metals, it is well known that the adsorption behavior of the thiophene molecule depends on the coverage and the temperature because of differences in the competitive bonding of the S-lone pair and the π-aromatic ring orbitals [4,5,17,45–47]. On a noble-metal surface like Cu(1 1 1) [46] or Ag(1 1 1) [47], it was found that thiophene undergoes a structural phase transition as a function of coverage. The same phenomenon could be responsible for the complex TDS data in Fig. 1. Our DF calculations in Section 3.2 indicate that at low coverages of thiophene, bonding through the ring is the most stable adsorption configuration, but as the adsorbate coverage increases bonding via S becomes competitive.

Fig. 2 displays photoemission C 1s core-level spectra for the adsorption of C_4H_4S on an almost stoichiometric TiO_2(1 1 0) surface. C_4H_4S was adsorbed at 100 K followed by heating to the indicated temperature. From 0.1 to 1.75 ML coverages, the C 1s intensity is gradually increased. Only one C 1s peak is seen in Fig. 2, with the binding energy located at ~285.2–285.4 eV. Upon dosing 1.75 ML, the BE value is 285.3 eV, which is in good agreement with the C 1s values of a C_4H_4S multilayer on Ag(1 1 1) [48]. Heating to 150 K causes a rapid decrease in the intensity of the multilayer features. A little shift (~0.15 eV) of C 1s is seen. This shift may be due to desorption of physisorbed C_4H_4S. By 300 K, most of the C species have disappeared from the surface, consistent with the TDS results in Fig. 1. Heating up to 450 K completely removes the C species from the surface. No atomic C signal is observed up to 800 K. Fig. 3 shows the corresponding S 2p data for the experiments in Fig. 2. Only an ill-defined doublet appears after an exposure of 0.1 ML, with a S $2p_{3/2}$ peak at ~164.5 eV. From 0.1 to 1.75 ML, the S 2p intensity is gradually increased. At a dose of 1.75 ML, the S $2p_{3/2}$ peak is located at ~165 eV, near the reported S $2p_{3/2}$ BE value for physisorbed C_4H_4S on Ag(1 1 1) [48], 164.8 eV. Heating to 150 K drastically reduces the S 2p intensity. By 300 K, almost no sulfur exists on the surface, consistent with the C 1s results shown in Fig. 2. In summary, for C_4H_4S on almost stoichiometric TiO_2(1 1 0) surfaces, the adsorption and desorption process is reversible.

On titania surfaces, reproducible populations of oxygen vacancies can be generated by heavy ion bombardment with Ar^+ or Ne^+ [19,23]. These oxygen vacancies are associated with cations of lower oxidation states like Ti^{3+} or Ti^{2+} [19]. The TiO_2(1 1 0) surface morphology becomes rough and disordered upon sputtering, as imaged by scanning tunneling microscopy (STM) [49]. Fig. 4 displays the Ti 2p photoemission spectra for an almost stoichiometric surface and a defective surface, respectively. Ne^+ sputtering leads to the appearance of a shoulder on

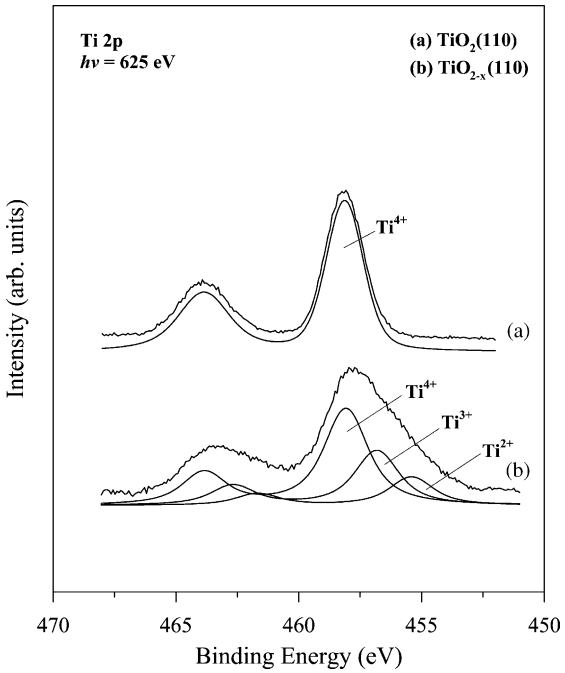

Fig. 4. Ti 2p spectra of (a) an almost stoichiometric TiO_2(1 1 0) surface; and (b) TiO_{2-x}(1 1 0) surface with a 45% concentration of "$Ti^{\delta+}$" ($\delta = 3, 2$). The spectra were obtained using a photon energy of 625 eV.

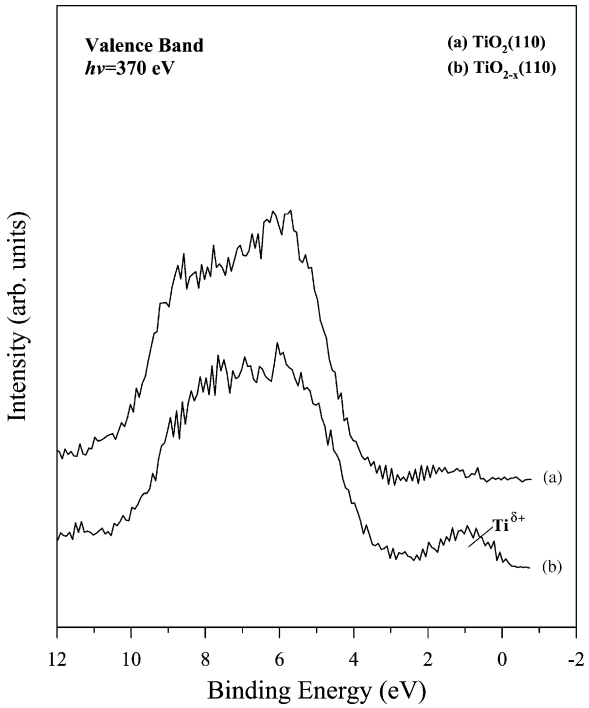

Fig. 5. Valence band photoemission for (a) TiO_2(1 1 0); and (b) TiO_{2-x}(1 1 0) surfaces as shown in Fig. 4. The spectra were obtained using a photon energy of 370 eV.

the low binding energy side. The curve fitting [50] results for this type of system reveal the existence of three oxidation states, which can be assigned to Ti^{4+}, Ti^{3+}, and Ti^{2+} cations, with the relative concentration (determined by XPS peak area) of Ti^{3+} and Ti^{2+} close to 45% of all the Ti sites. The valence band spectrum shown at the bottom of Fig. 5 supports the core-level results. The deficiency of oxygen on the TiO_2(1 1 0) surfaces leads to a state (mainly derived from Ti^{3+} cations [22,23]) within the band gap at a binding energy of ~1 eV. The valence band features and the BE value of the "defect state" in Fig. 5 are similar to those of previous data obtained with ultraviolet photoelectron spectroscopy (UPS) [23]. The "defect state" plays a key role in the dissociation of SO_2 and CH_3SH on TiO_{2-x}(1 1 0) [19,24], and it is worthwhile to establish if the same could occur for the adsorption of thiophene.

The interaction of C_4H_4S with a TiO_{2-x}(1 1 0) surface containing a high concentration of defects (as shown in Figs. 4 and 5) was also investigated. Fig. 6 displays the changes in C 1s core-level spectra after increasing the dosing amount of thiophene from 0.1 to 1.3 ML at 100 K, followed by stepwise heating up to 800 K. For 0.1 ML dosing, two C 1s features are seen, located at ~285.2 and ~282.5 eV. The C 1s region is dominated by the peak at ~285.2 eV, with a small contribution from the peak at ~282.5 eV (corresponding to 0.01 ML). From 0.1 to 1.3 ML, the C 1s core-level feature at 285.2 eV is gradually increased in intensity, and the C 1s feature at 282.5 eV remains constant. According to the results for C_4H_4S on the almost stoichiometric TiO_2(1 1 0) surface (shown in Fig. 2), the C 1s feature at 285.2 eV is attributed to the intact C_4H_4S molecules. The C 1s feature at 282.5 eV is typical for decomposed hydrocarbon species on the surface, denoted as C_x [19]. Heating to 150 K significantly decreases the intensity for the intact C_4H_4S molecules due to desorption of the physisorbed multilayer (see above). By 300 K, only a very small amount of C 1s signal remains in the spectrum. The C_x species is seen

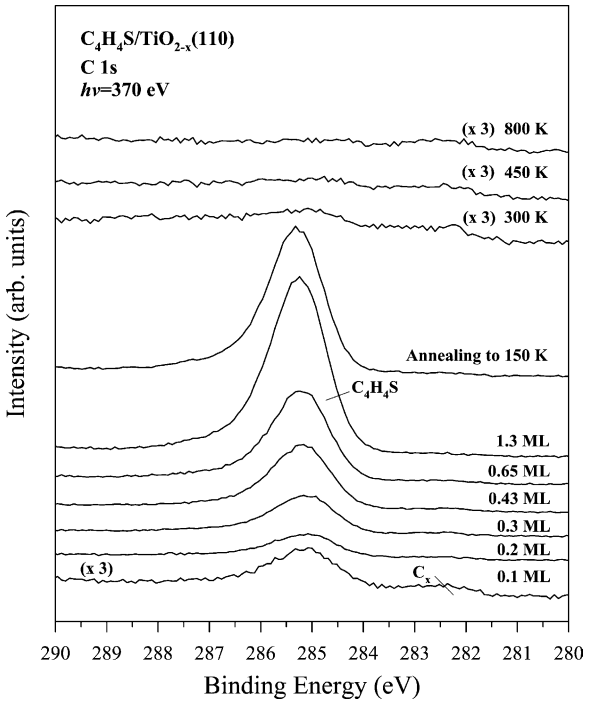

Fig. 6. C 1s spectra ($h\nu = 370$ eV) for the adsorption of C_4H_4S on a reduced TiO_{2-x}(1 1 0), as shown in Fig. 4(b). C_4H_4S was dosed at 100 K, and the surface was annealed to the indicated temperatures.

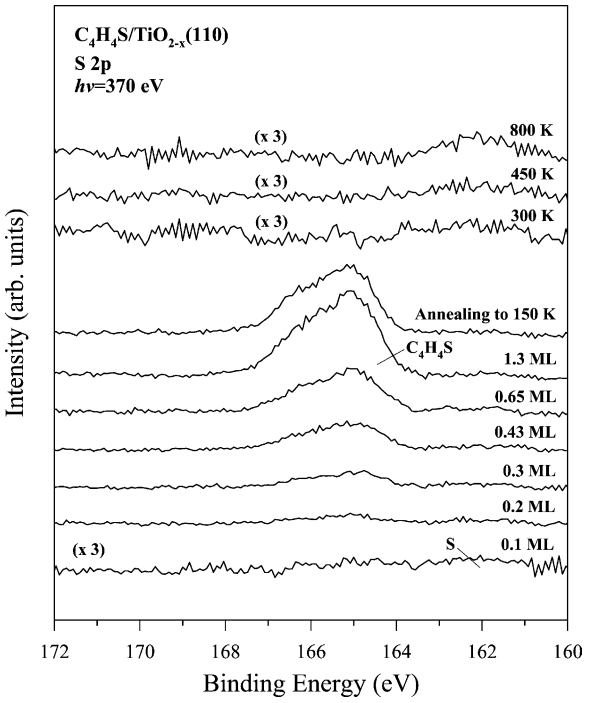

Fig. 7. S 2p spectra ($h\nu = 370$ eV) for the adsorption of C_4H_4S on the TiO_{2-x}(1 1 0) surface of Fig. 6. C_4H_4S was dosed at 100 K, and the surface annealed to the indicated temperatures.

on the surface up to 800 K. The corresponding S 2p core-level spectra are shown in Fig. 7. At 0.1 ML dosing, only a trace of sulfur-containing species is seen at ~162 eV, which is a typical BE value for atomic sulfur [19], indicating the decomposition of the parent C_4H_4S molecules. For a larger dose of 0.2 ML, a second peak starts to grow at ~165 eV, assigned to the intact C_4H_4S molecules. From 0.1 to 1.3 ML, the peak intensity at 165 eV gradually increases, without noticeable changes in the BE value. Heating to 150 K removes the multilayer, and by 300 K, the parent signal almost disappears from the S 2p spectrum. The atomic sulfur feature still exists up to 800 K, consistent with previous studies [19,32]. The present results show a limited decomposition of C_4H_4S molecules on a defective titania surface.

Fig. 8 shows TDS spectra for thiophene adsorption on defective TiO_{2-x}(1 1 0) surfaces. The generated defect concentration by ion sputtering was close to that of the TiO_{2-x}(1 1 0) surfaces in Figs. 4 and 5. At 0.75 ML coverage, a broad desorption feature is seen with a desorption peak α at 170 K. Due to the roughness of the TiO_{2-x}(1 1 0) surfaces, all of the well-defined desorption states seen in Fig. 1 for thiophene/TiO_2(1 1 0) are not present in Fig. 8. For adsorption of 1.15 ML, a second desorption peak, denoted as β, is observed at 140 K. The β peak, which was not saturated with large doses of thiophene, is assigned as desorption from a condensed physisorbed layer. No other hydrogen-containing products (H_2, C_4H_6, and C_4H_8) and sulfur-containing species (S, S_2, and SO_2) were detected in TDS. However, the TDS experiments may be insensitive to a very small amount of decomposed thiophene observed via XPS. The hydrogen produced by the decomposition reaction could diffuse into the bulk of the oxide as proposed in another studies [51,52]. The lack of dissociation of thiophene on TiO_{2-x}(1 1 0) is interesting, and in the next section we will examine the interaction of O vacancies with thiophene in detail using DF calculations.

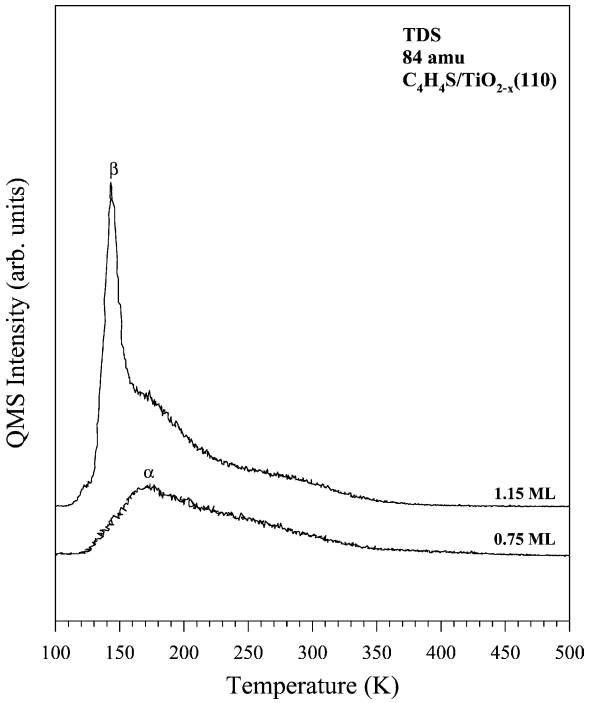

Fig. 8. Thermal desorption spectra for thiophene adsorption on a defective TiO_{2-x}(1 1 0) surface (∼45% of "$Ti^{\delta+}$" centers, $\delta = 3, 2$) at 100 K as a function of relative monolayer coverage. The ion signal (84 amu) was monitored. The heating rate (dT/dt) was 2 K/s.

3.2. Bonding of thiophene to TiO_2(1 1 0) and TiO_{2-x}(1 1 0): density-functional studies

Following previous studies [19,32], the TiO_2(1 1 0) surface was represented by a four-layer slab as shown in the top of Fig. 9, which was embedded in a three-dimensionally periodic supercell [31]. A vacuum of 15 Å was placed on top of the slab in order to ensure negligible interactions between periodic images normal to the surface [19,31,32]. The geometry optimization for bulk TiO_2 gave a rutile unit cell with $a = b = 4.64$ Å and $c = 2.97$ Å. These values are close to those derived from experimental measurements ($a = b = 4.59$ Å, $c = 2.96$ Å) [53] and other theoretical calculations [32]. In the slab calculations the structural geometry of the first two layers was relaxed, while the other two layers were kept fixed in the geometry of bulk TiO_2. For the perfect TiO_2(1 1 0) surface, the five-fold and six-fold coordinated Ti ions moved in and out of plane by 0.15 and 0.11 Å,

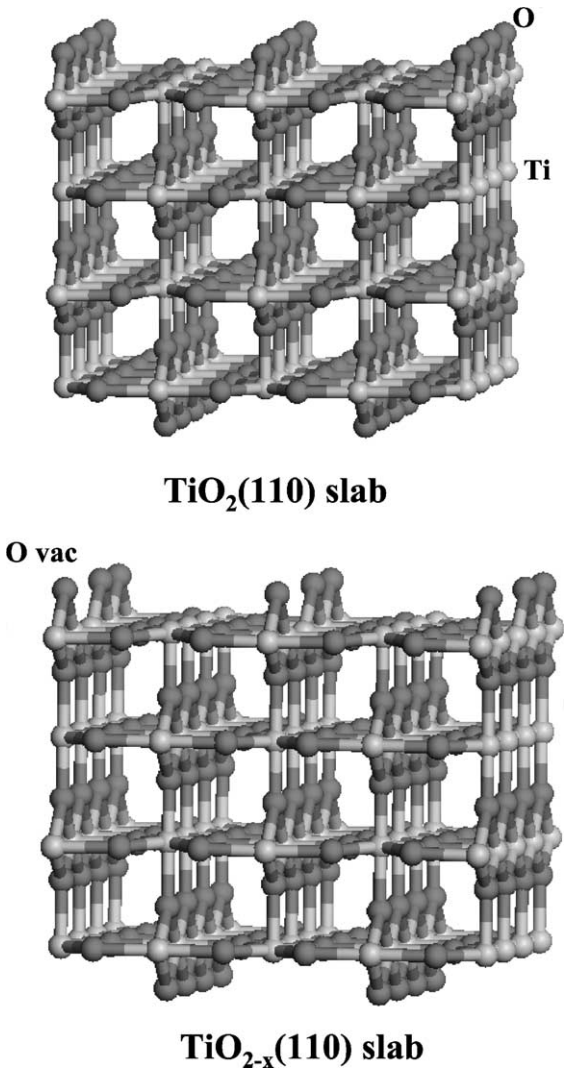

Fig. 9. Four-layer Slab models used to describe perfect, top, and O-vacancy rich, bottom, TiO_2(1 1 0) surfaces. In the TiO_{2-x}(1 1 0) slab, the O vacancies are present only on the top layer in a $p(4\times1)$ array. Dark spheres represent O atoms, while white spheres correspond to Ti atoms.

respectively. The bridging oxygens moved into the surface by 0.10 Å, and the in-plane oxygens moved out of the surface by 0.11 Å. These shifts in the atom positions agree well with those seen in other DF studies [33]. Most of them are also in good agreement with atomic shifts found in X-ray surface diffraction studies for TiO_2(1 1 0) [54], the only exception being the shift for the bridging oxygens where the experi-

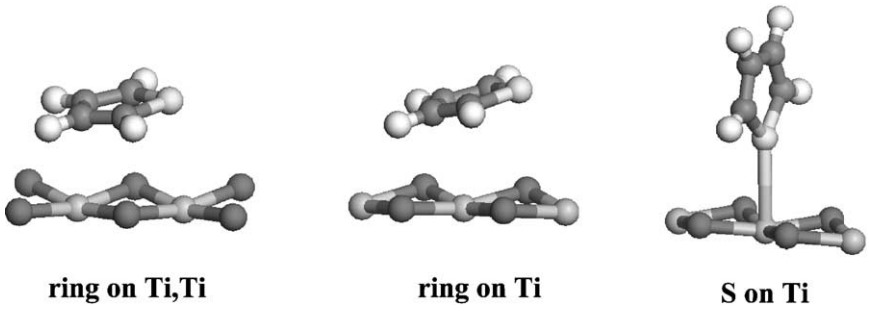

Fig. 10. Bonding configurations for thiophene on $TiO_2(1\,1\,0)$.

mental results give a movement of 0.27 Å towards the surface.

Based on previous studies [4,5,15,55], we examined bonding of the molecule through its S-end or via the aromatic ring. Fig. 10 shows the three most stable configurations found in the DF calculations. They mainly involve bonding to the Ti cations of the surface. Table 1 lists adsorption energies and geometries obtained for thiophene coverages of 0.25 ML, $p(4\times1)$ overlayer, and 0.5 ML, $p(2\times1)$ overlayer. In the calculations, the geometry of the adsorbate and the first two layers of the slab were allowed to relax. According to

Table 1
Adsorption of thiophene on $TiO_2(1\,1\,0)$ terraces: DF-GGA results

Bonding configuration	Adsorption energy (kcal/mol)	C–S bond length[a] (Å)	S–Ti bond length (Å)
Ring on Ti, Ti	12 (5)[b]	1.70 (1.69)	3.41 (3.63)
Ring on Ti	11 (5)	1.69 (1.69)	3.68 (3.92)
S on Ti	8 (7)	1.69 (1.69)	2.78 (2.86)

[a] 1.69 Å for free thiophene.

[b] The values in parentheses correspond to a thiophene coverage of 0.5 ML. The numbers outside the parentheses are for a coverage of 0.25 ML.

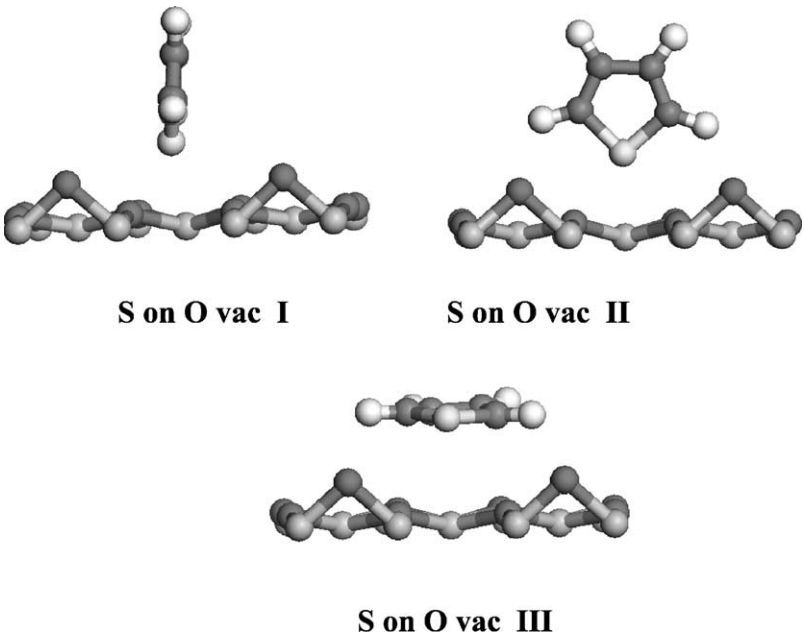

Fig. 11. Bonding configurations for thiophene on $TiO_{2-x}(1\,1\,0)$.

the calculations, thiophene should bond with its aromatic ring nearly parallel to the surface at the smaller coverage. The molecule could be bridging atoms in the Ti rows. As the thiophene coverage increases, there is a decrease in the adsorption energy and bonding through the S atom becomes more stable; partly because this diminishes adsorbate ↔ adsorbate repulsion on the surface. In any case, even at low coverage of thiophene, the bonding interactions with the oxide surface are relatively weak and the adsorption of the molecule has a negligible effect on the strength of the C–S bonds.

The bottom of Fig. 9 shows the slab used to model the adsorption of thiophene on O vacancies of TiO_{2-x}(1 1 0). In this system, 25 % of the atoms in the bridging O rows of the first layer are missing (a concentration that is consistent with the amount of defects in the experiments of Figs. 4–8). The O vacancies form a $p(4 \times 1)$ array. In many situations it is unlikely that O vacancies in TiO_2 will assume a periodic array such as shown in Fig. 9, but such model represents well electronic and chemical perturbations associated with the formation of O vacancies [19,24,32,50]. On the O vacancies, we found that bonding of thiophene via S (Fig. 11) was more stable than via H or C. For 0.25 ML of thiophene on the TiO_{2-x}(1 1 0) surface, the molecular adsorption energy was 15–17 kcal/mol for the configurations shown in Fig. 11. These bonding energies are larger than those found on a perfect TiO_2(1 1 0) surface, but upon adsorption on TiO_{2-x}(1 1 0) the elongation of the C–S bonds was less than 0.02 Å, with a negative charge on the molecule of less than 0.10*e*. These results indicate that the interaction between the vacancy states of TiO_{2-x}(1 1 0) and the LUMO of thiophene (C–S antibonding [55]) is weak.

4. Discussion

For industrial applications, the most widely used metal catalysts are supported on high surface area materials, i.e. oxide powders [2]. In general, the role of catalyst supports can be complex and they can offer high surface area for particle dispersion and/or strong interactions at metal-oxide interfaces [2,23]. In spite of the use of oxides as sorbents or catalysts in desulfurization applications [2,26], very few studies have been published examining the interaction of thiophene and pure oxide surfaces [15,16]. The surface chemistry of thiophene on polycrystalline γ-Al_2O_3 powders has been investigated after the condensation of a multilayer at 130 K [16]. In addition to reversible adsorption and desorption, only two peaks were displayed in TDS spectra with maximum rates of desorption at 175 and 220 K for multilayer thiophene and weakly chemisorbed thiophene [16]. Thiophene interacts only weakly with the alumina and no decomposition was observed upon heating to 600 K under UHV conditions or under a 3.0 Torr partial pressure of thiophene [16]. Previous studies [49,56] show that Ar^+ sputtering can increase the surface area by creating disordered structures on TiO_2 surfaces. The similar TDS results on defective TiO_{2-x}(1 1 0) and γ-Al_2O_3 powders show the effect of surface morphology on the thiophene bonding modes and/or adsorption sites. Neither of these rough surfaces is able to dissociate thiophene.

The fact that the TDS features for thiophene on the defective titania are different from those of the almost stoichiometric titania implies the presence of different adsorption sites on these two surfaces. On an almost stoichiometric TiO_2(1 1 0) surface, well-defined desorption peaks are seen in Fig. 1. TDS spectra exhibit multiple desorption states for thiophene adsorption on noble metals such as Au(1 1 1) [17], Cu(1 1 1) [46], and Ag (1 1 1) [47]. It is well known that thiophene can adopt either flat or tilted adsorption geometries via its π-clouds or S-lone pair of electrons, respectively [17,46,47]. Depending on the coverages, changes in the bonding geometries and structural phase transitions occur [46,47]. The complex desorption states in Fig. 1 could be attributed to several different adsorption conformations for thiophene on titania. Our DF calculations indicate that the molecule should be bonded through the S-end on O-vacancy sites. On terraces of TiO_2(1 1 0), adsorption via the π-cloud of the ring should occur at low coverages, with bonding through the S atom lone pair at high coverage. Infrared studies for thiophene on γ-Al_2O_3 powders [16] have shown three different adsorption configurations for the molecule. One of them could be identified, and corresponded to a thiophene species bonded to Al^{3+} cations via S.

MoS_x/TiO_2 systems are active catalysts for HDS reactions [27–29]. These systems display an HDS activity that is ∼5 times higher than that of MoS_x/Al_2O_3

catalysts where alumina is just a support that facilitates the dispersion of MoS_2 [1,27]. The high HDS activity of MoS_x/TiO_2 could be a consequence of the presence of Ti^{3+} sites within the oxide [29]. For thiophene on almost stoichiometric titania we saw no dissociation, as has been observed previously on zinc oxide [15] and alumina [16]. For metal sulfides, the creation of S vacancies leads to coordinatively unsaturated metal cations and an increase in the HDS activity [12,55,57–61]. In principle, one would expect that something similar could occur in an oxide like TiO_2 after forming Ti^{3+} sites by the removal of oxygen [29,62,63]. Our experimental and theoretical studies show that such Ti^{3+} sites in $TiO_{2-x}(1\,1\,0)$ are not very active for the dissociation of the molecule. For defective surfaces of $TiO_{2-x}(1\,1\,0)$ with 45% $Ti^{\delta+}$ (Ti^{3+} and Ti^{2+}), only a small fraction (<0.05 ML, determined by XPS peak area) of the adsorbed thiophene molecules decomposed. From these data, we can conclude that Ti^{3+} centers in MoS_x/TiO_2 may not be direct active sites for HDS reactions. However, the Ti^{3+} could act as an "electronic promoter" for the active molybdenum sulfide phase as proposed in previous works [29,63]. For example, in Au/TiO_2 catalysts for the destruction of SO_2 [24], interaction with Ti^{3+} centers enhances the activity of the supported gold nanoparticles. Recent results [63] indicate that Ti^{3+} species could play a promoting role in the HDS activity of molybdenum sulfide, in the same way as Co and Ni promoters. In principle, an electron transfer from Ti^{3+} to the Mo 3d conduction band could occur, and lead to weak Mo–S bonds [29,63] opening in this way the Mo cations for HDS reactions. This is a topic that needs additional studies to be confirmed or rejected. Also Ti^{3+} sites could help in the dissociation of H_2 [29,64], which then will spill-over onto sites on Mo sulfide to be used in desulfurization reactions.

In general, O vacancies enhance the reactivity of $TiO_2(1\,1\,0)$ towards S-containing molecules [19,24,32] and other adsorbates [23,65]. Even in the case of SO_2, the Ti^{3+} centers readily cleavage the double bonds between S and O [24]. Thus, the lack of dissociation seen in the thiophene/$TiO_{2-x}(1\,1\,0)$ system must be attributed to the high stability of the aromatic ring in the adsorbate. In thiophene the LUMO appears very high in energy [55] and interacts poorly with the vacancy states of $TiO_{2-x}(1\,1\,0)$. For adsorption on the O vacancies, the calculated negative charges on S ($-0.3e$ [32]), CH_3S ($-0.2e$ [19]) and SO_2 ($-0.5e$ [24]) were more substantial than in thiophene ($-0.06e$). Theoretical calculations for the bonding of thiophene to ZnO clusters also show a negligible charge on the molecule ($\sim 0.05e$ [15]). The typical ionicity of oxides leads to metal centers with a high positive charge and a low density of states near the Fermi level [23]. The net result are poor bonding interactions between an oxide and the LUMO of thiophene. Surfaces that are able to transfer electrons into this orbital have no problems dissociating the molecule [4–6,15,55,66]. Thus, C_4H_4S readily decomposes on most metal surfaces [4–7].

5. Conclusions

In this paper, the adsorption of C_4H_4S on almost stoichiometric $TiO_2(1\,1\,0)$ and defective $TiO_{2-x}(1\,1\,0)$ surfaces has been studied with a combination of synchrotron-based high-resolution photoemission spectroscopy, TDS, and first-principles DF slab calculations. Over an almost stoichiometric $TiO_2(1\,1\,0)$ surface, the adsorption and desorption of C_4H_4S is completely reversible. No thiophene decomposition was observed up to 800 K under ultra-high vacuum conditions. In the submonolayer regime, four adsorption states in the temperature range of 150–450 K were identified in TDS. Very weak desorption features at 320 and 450 K can be attributed to thiophene adsorption on defects and steps of the surface. Thiophene bonded to terraces of $TiO_2(1\,1\,0)$ desorbs at temperatures below 300 K. The results of DF calculations indicate that at small coverage the molecule is bonded with its ring nearly parallel to the surface. At high coverages of thiophene, bonding through the S atom becomes more stable. On a defective $TiO_{2-x}(1\,1\,0)$ surface with ~45 % of Ti^{3+} and Ti^{2+}, a small fraction of the adsorbed thiophene molecules (<0.05 ML) decomposed. Our experimental and theoretical studies indicate that the vacancy states of $TiO_{2-x}(1\,1\,0)$ interact poorly with the LUMO of thiophene. This is a behavior opposite to that found for the adsorption of S_2, CH_3S and SO_2. Our results are consistent with the idea that the Ti^{3+} centers in MoS_x/TiO_2 catalysts are not the direct active sites for HDS reactions, but maybe "electronic promoters" for the active molybdenum sulfide phase.

Acknowledgements

The authors at Brookhaven National Laboratory thank the financial support of the US Department of Energy (DOE), Division of Chemical Sciences under the contract of DE-AC02-98CH10886. The NSLS is supported by the Division of Materials and Chemical Sciences of DOE.

References

[1] H. Topsøe, B. Clausen, F.E. Massoth, in: J.R. Anderson, M. Boudart (Eds.), Catalysis: Science and Technology, vol. 11, Springer, Berlin, 1996, p. 1.
[2] C.N. Satterfield, Heterogeneous Catalysis in Industrial Practice, McGraw-Hill, New York, 1991.
[3] A.C. Stern, R.W. Boubel, D.B. Turner, D.L. Fox, Fundamentals of Air Pollution, second ed., Academic Press, New York, 1994.
[4] C.M. Friend, D.A. Chen, Polyhedron 16 (1997) 3165.
[5] F. Zaera, E.B. Kollin, J.L. Gland, Surf. Sci. 184 (1987) 75.
[6] J.A. Rodriguez, J. Dvorak, T. Jirsak, Surf. Sci. 457 (2000) L413.
[7] A.J. Gellman, M.E. Bussell, G.A. Somorjai, J. Catal. 107 (1987) 103.
[8] T.E. Galdwell, I.M. Abdelrehim, D.P. Land, Surf. Sci. 367 (1996) L26.
[9] D.R. Huntley, D.R. Mullins, M.P. Wingeier, J. Phys. Chem. 100 (1996) 19620.
[10] R. Prins, V.H.J. De Beer, G.A. Somorjai, Catal. Rev. Sci. Eng. 31 (1989) 1.
[11] M.J. Ledoux, O. Michaux, G. Agostini, P. Pannisod, J. Catal. 102 (1986) 275.
[12] T.L. Tarbuck, K.R. McCrea, J.W. Logan, J.L. Heiser, M.E. Bussell, J. Phys. Chem. B 102 (1998) 7845.
[13] P. Mills, D.C. Phillips, B.P. Woodruff, R. Main, M.E. Bussell, J. Phys. Chem. B. 104 (2000) 3237.
[14] J.A. Rodriguez, J. Dvorak, A.T. Capitano, A.M. Gabelnick, J.L. Gland, Surf. Sci. 429 (1999) L462 (and references therein).
[15] T. Jirsak, J. Dvorak, J.A. Rodriguez, J. Phys. Chem. B 103 (1999) 5550.
[16] W.W.C. Quigley, H.D. Yamamoto, P.A. Aegerter, G.J. Simpson, M.E. Bussell, Langmuir 12 (1996) 1500.
[17] G. Liu, J.A. Rodriguez, J. Dvorak, J. Hrbek, T. Jirsak, Surf. Sci. 505 (2002) 295.
[18] H. Yamamoto, R.A. Butera, Y. Gu, D.H. Waldeck, Langmuir 15 (1999) 8640.
[19] G. Liu, J.A. Rodriguez, Z. Chang, J. Hrbek, L. González, J. Phys. Chem. B 106 (2002) 9883.
[20] F. Schreiber, Prog. Surf. Sci. 65 (2000) 151.
[21] J. Noh, K. Kobayashi, H. Lee, M. Hara, Chem. Lett. (2000) 630.
[22] J. Noh, E. Ito, K. Nakajima, J. Kim, H. Lee, M. Hara, J. Phys. Chem. B 106 (2002) 7139.
[23] V.E. Henrich, P.A. Cox, The Surface Science of Metal Oxides, Cambridge University Press, Cambridge, 1994.
[24] J.A. Rodriguez, G. Liu, T. Jirsak, J. Hrbek, Z. Chang, J. Dvorak, A. Maiti, J. Am. Chem. Soc. 124 (2002) 5242.
[25] E. Farfan-Arribas, R.J. Madix, J. Phys. Chem. B 106 (2002) 10680.
[26] A. Pieplu, O. Saur, J.-C. Lavalley, O. Legendre, C. Nedez, Catal. Rev.-Sci. Eng. 40 (1998) 409.
[27] J. Ramirez, S. Fuentes, G. Diaz, M. Vrinat, M. Breysse, M. Lacroix, Appl. Catal. 52 (1989) 211.
[28] C. Pophal, F. Kameda, K. Hoshino, S. Yoshinata, K. Segawa, Catal. Today 39 (1997) 21.
[29] J. Ramirez, L. Cedeno, G. Busca, J. Catal. 184 (1999) 59.
[30] V. Milman, B. Winkler, J.A. White, C.J. Pickard, M.C. Payne, E.V. Akhmatskaya, R.H. Nobes, Int. J. Quantum Chem. 77 (2000) 895.
[31] M.C. Payne, D.C. Allan, T.A. Arias, J.D. Johannopoulus, Rev. Mod. Phys. 64 (1992) 1045.
[32] J.A. Rodriguez, J. Hrbek, Z. Chang, J. Dvorak, T. Jirsak, A. Maiti, Phys. Rev. B 65 (2002) 235414.
[33] D.C. Sorescu, J.T. Yates, J. Phys. Chem. B 102 (1998) 4556.
[34] D.C. Sorescu, C.N. Rusu, J.T. Yates, J. Phys. Chem. B 104 (2000) 4408.
[35] K. Refson, R.A. Wogelius, G. Fraser, M.C. Payne, M.H. Lee, V. Milman, Phys. Rev. B 52 (1995) 10823.
[36] J.A. Rodriguez, J.C. Hanson, S. Chaturvedi, A. Maiti, J.L. Brito, J. Chem. Phys. 112 (2000) 935.
[37] J.A. Rodriguez, T. Jirsak, M. Pérez, L. González, A. Maiti, J. Chem. Phys. 114 (2001) 4186.
[38] D. Vanderbilt, Phys. Rev. B 41 (1990) 7892.
[39] H.J. Monkhorst, J.D. Pack, Phys. Rev. B 13 (1976) 5188.
[40] J.A. White, D.M. Bird, Phys. Rev. B 50 (1994) 4954.
[41] J.P. Perdew, K. Burke, Y. Wang, Phys. Rev. B 54 (1996) 16533.
[42] M.D. Segall, C.J. Pickard, R. Shah, M.C. Payne, Phys. Rev. B 54 (1996) 16317.
[43] J. Hrbek, J.A. Rodriguez, J. Dvorak, T. Jirsak, Collect. Czech. Chem. Commun. 66 (2001) 1149.
[44] D. Brinkley, T. Engel, J. Phys. Chem. B 104 (2000) 9836.
[45] J.P. Fulmer, F. Zaera, W.T. Tysoe, J. Phys. Chem. 92 (1988) 4147.
[46] P.K. Milligan, B. Murphy, D. Lennon, B.C.C. Cowie, M. Kadodwala, J. Phys. Chem. B 105 (2001) 140.
[47] P. Väterlein, M. Schmelzer, J. Taborski, T. Krause, F. Viczian, M. Bäßler, R. Fink, E. Umbach, W. Wurth, Surf. Sci. 452 (2000) 20.
[48] K.M. Baumgärtner, M. Volmer-Uebing, J. Taborski, P. Bäuerle, E. Umbach, Ber. Bunsen-Ges. Phys. Chem. 95 (1991) 1488.
[49] A. Szabo, T. Engel, Surf. Sci. 329 (1995) 241.
[50] J.A. Rodriguez, T. Jirsak, G. Liu, J. Hrbek, J. Dvorak, A. Maiti, J. Am. Chem. Soc. 123 (2001) 9597.
[51] L. Gamble, L.S. Jung, C.T. Campbell, Surf. Sci. 348 (1996) 1.
[52] E. Farfan-Arribas, R.J. Madix, J. Phys. Chem. B 106 (2002) 10680.

[53] S.C. Abrahams, J.L. Bernstein, J. Chem. Phys. 55 (1971) 3206.
[54] G. Charlton, P.B. Howes, C.L. Nicklin, P. Steadman, J.S.G. Taylor, C.A. Muryn, S.P. Harte, J. Mercer, R. MacGrath, D. Norman, T.S. Turner, G. Thorton, Phys. Rev. Lett. 78 (1997) 495.
[55] J.A. Rodriguez, J. Phys. Chem. B 101 (1997) 7524.
[56] L.Q. Wang, K.F. Ferris, J.P. Winokur, A.N. Shultz, D.R. Bare, M.H. Engelhard, J. Vac. Sci. Technol. A 16 (1998) 3034.
[57] M. Salmeron, G.A. Somorjai, A. Wold, R. Chianelli, K.S. Liang, Chem. Phys. Lett. 90 (1982) 105.
[58] B. Müller, A.D. van Langeveld, J.A. Moulijn, H. Knözinger, J. Phys. Chem. 97 (1993) 105.
[59] J.A. Rodriguez, J. Dvorak, T. Jirsak, S.Y. Li, J. Hrbek, A.T. Capitano, A.M. Gabelnick, J.L. Gland, J. Phys. Chem B 103 (1999) 5550.
[60] L.S. Byskov, B. Hammer, J.K. Nørskov, B.S. Clausen, H. Topsøe, Catal. Lett. 47 (1997) 177.
[61] A.N. Startsev, Catal. Rev.-Sci. Eng. 37 (1995) 353.
[62] D. Wang, W. Qian, A. Ishihara, T. Kabe, Appl. Catal. A 224 (2002) 191.
[63] L. Coulier, J.A.R. van Veen, J.W. Niemantsverdret, Catal. Lett. 79 (2002) 149.
[64] G. Rocker, W. Göpel, Surf. Sci. Lett. 175 (1986) L675.
[65] M.A. Barteau, Chem. Rev. 96 (1996) 1413.
[66] J.A. Rodriguez, Surf. Sci. 278 (1992) 326.